# Comparative Study on Connection Properties of Shear Bolt and Screw of Thin Cross-laminated Timber Panel

Daiyuan Zhang,[a] Liming Shen,[a,*] Xudong Zhu,[a,b] Sujun Zhang,[b] Meng Gong,[c] and Yuewen Gao [b]

Cross-laminated timber (CLT), a wood product with excellent shear resistance, is often used in modern timber constructions. Using the standards ASTM D1761-12 (2020) and NDS-2012 (2012), this study investigated the connection properties of shear bolts and screws in CLT panels. The specimens were made from spruce-pine-fir lumber and installed on a test platform using one high-strength bolt or eight screws, and then an upward load was applied to the top of the specimen. The results showed that the bolt connection provided a higher ultimate bearing capacity and elastic stiffness. The bolt exhibited virtually no deformation, and the CLT panel did not noticeably deteriorate when the connection was damaged. The distance between the bolt hole and the bottom of the CLT specimen and the angle between the outer-layer grain direction of the CLT panel and the load direction were both measured. Changes in the ductility coefficient value had an obvious effect on the connection performance of the shear bolts when the outer-layer grain direction of the CLT panel was consistent with the load direction. Contrastingly, when the outer-layer grain direction of the CLT panel was perpendicular to the load direction, the effect was negligible, and the yield load was nearly unchanged.

*DOI: 10.15376/biores.18.1.827-843*

*Keywords: Cross-laminated timber; Connection properties; Bolt; Screw*

*Contact information: a: College of Science and Engineering, Nanjing Forestry University, Nanjing 210037 China; b: Yangzhou Polytechnic Institute, Jiangsu 225200 China; c: Wood Science and Technology Centre, University of New Brunswick, 1350 Regent St., Fredericton E3C 2G6 Canada;*
** Corresponding author: shenlimingda@hotmail.com*

## INTRODUCTION

At present, reducing carbon emissions is a major objective of the international community. The construction industry accounts for up to 30% of the world’s annual greenhouse gas emissions (IEA 2019). Therefore, reducing this sector’s carbon footprint is crucial for mitigating climate change. One solution is building houses from wood because wood is a natural building material that stores carbon. However, it is difficult for traditional light timber structure buildings to meet the requirements of high-rise buildings in terms of fire performance and structural strength. Cross-laminated timber (CLT) is a novel engineered wood material that was originally developed by scientists in Germany and Austria (Schickhofer and Guggenberger 1994). This material is made of multiple mutually perpendicular layers of wood. Timber structure buildings with CLT panels as the main structural components have good fire performance, structural strength, and lateral stiffness. Many countries are currently promoting CLT mid- and high-rise timber structure buildings on a large scale (Frangi *et al.* 2008; Frangi *et al.* 2009; Klippel *et al.* 2014; Wang *et al.* 2015; Brandner *et al.* 2016; Sikora *et al.* 2016). Cross-laminated timber structures constitute a new type of building suitable for assembly construction. Therefore, the connection mode in CLT structures is an important research topic. In common CLT buildings, CLT wall panels and floors are mainly connected using hold-down fasteners and wood screws. Although this connection mode is convenient for assembly, it is susceptible to considerable nail connection damage under transverse loads, which drastically reduces the overall lateral stiffness of CLT wall systems; this is mainly manifested by the bending or pulling out of wood screws under lateral loads, as well as the sliding displacement of the overall wall panel (Varoḡlu *et al.* 2007; Wei *et al.* 2015). In general, the performance of traditional light-frame timber shear walls is primarily determined by the response of the nail connection rather than the properties of the timber members (Dinehart and Shenton, III 2000; Richard *et al.* 2002; Li *et al.* 2012, 2015; Verdret *et al.* 2015). Compared with light-frame timber walls, CLT walls have a better lateral stiffness. Therefore, it is necessary to study better connection methods for CLT shear wall to avoid the overall stiffness reduction of wall systems because of improper connection methods. Cross-laminated timber panel and floor connection systems provide better overall stiffness by employing both side-angle steel and bolt penetrations through CLT panels.

The stiffness of bolted CLT wall systems is related to the bearing capacity of bolted joints. Current research on the bearing capacity of bolted joints in wood is based on the yield theory proposed by Johanson in 1941. Daudeville *et al.* (1999) conducted pin groove bearing tests to study the influence of the bolt diameter, edge distance, and end distance on the pin groove bearing strength. When the ratio of the wood thickness to the bolt diameter is small, the failure mode of a single-bolt or two-bolt connection tends to be brittle failure. Kharouf *et al.* (2005) conducted numerical simulations based on a nonlinear numerical model to study this failure mode. In their simulations, a compression plastic constitutive model was used in a certain area around the bolt. The resulting plastic deformation was in good agreement with experimental results obtained using glulam steel splint bolt connections (Kharouf *et al.* 2005). Considering the incompleteness of the bolt failure mode, especially the failure mode of group bolts, Moses and Prion (2003) proposed an anisotropic plastic model for wood and an ideal elastic-plastic model for bolts in view of the Canadian wood structure design standard CSA O86-14 (2019). In addition, the Weibull weakest link theory has been used to predict failure at given levels of probability (Moses and Prion 2003).

To investigate the application of screw and bolt connections in thin CLT panels in terms of the difference in shear performance, this study conducted shear tests involving four groups with two connection methods. The parameters studied included the section size, connection strength, shear stiffness, and failure mode of the specimens.

## EXPERIMENTAL

### Materials and Test Equipment

The spruce-pine-fir (SPF) lumber used in this study was purchased from Suzhou Jingxiu Construction Technology Co., Ltd. (Suzhou, China). It is a broad-grained wood, and the proportion of latewood is 25.7%. The average timber density is 0.48 g/cm$^3$. The timber was air-dried, after which its average moisture content was 9.65% at room temperature and humidity (23 °C and relative humidity of 65%). The SPF boards, 4000 mm in length (L), 89 mm in width (W), and 38 mm in thickness (T), were fabricated into 800 mm × 80 mm × 16 mm standard planks. Then, the planks were assembled *via* a cold press machine (XLB; Qingdao Guangyue Rubber Machinery Manufacturing Co., Ltd., Qingdao, China), and resin with a density of 200 g/m$^2$ was added between the layers. The resin was a common thermosetting one-component polyurethane (PUR) adhesive (PURBOND HB S709; Harbin Chengfeng Adhesive Co., Ltd., Harbin, China).

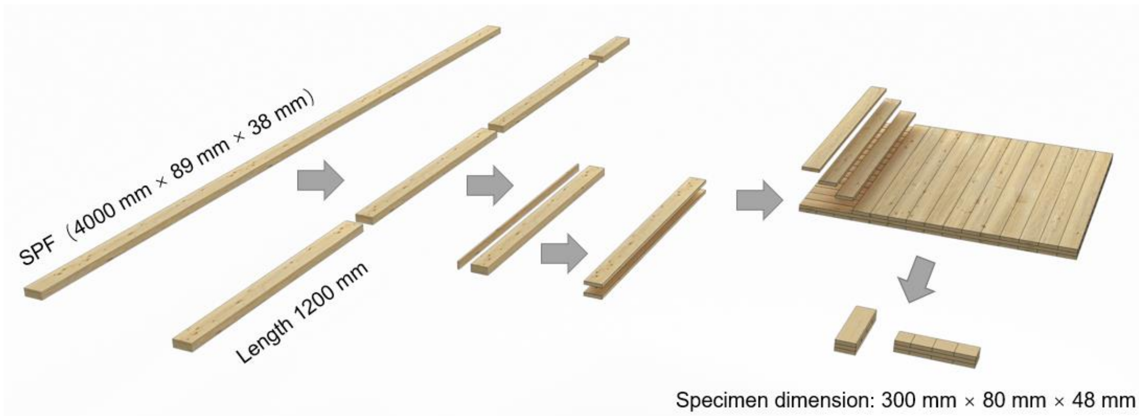


**Fig. 1.** Fabrication processes of the CLT samples

**Table 1.** Dimensions of Bolt Connection CLT Specimens

| Type | Distance Between Bolt Hole and Specimen Bottom (mm) | Angle Between Outer Wood Grain Direction and Load Direction (°) | Specimen Sketch |
|---|---|---|---|
| 1 | 40 | 0 | 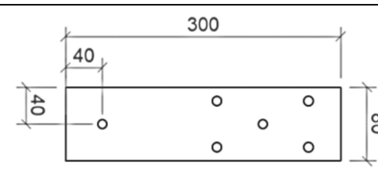  |
| 2 | 70 | 0 | 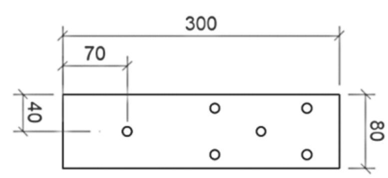  |
| 3 | 40 | 90 | 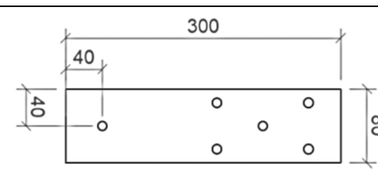  |
| 4 | 70 | 90 | 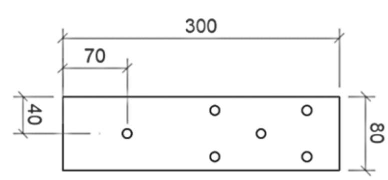  |

**Table 2.** Dimensions of Screw Connection CLT Specimens

| Type | Length of Screw (mm) | Angle Between Outer Wood Grain Direction and Load Direction (°) | Specimen Sketch |
|---|---|---|---|
| 5 | 60 | 0 | 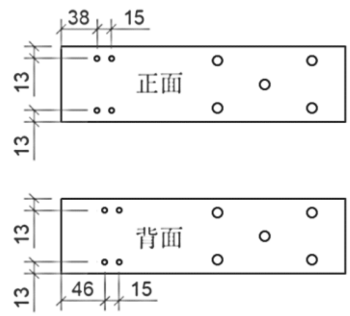 |
| 6 | 60 | 90 | |
| 7 | 40 | 0 | |
| 8 | 40 | 90 | |

The pressure of the cold press was maintained at 20 MPa for 8 to 12 h at a temperature of 15 °C. Subsequently, 1200 mm × 1200 mm × 48 mm three-layer CLT panels were obtained and trimmed into 300 mm × 80 mm × 48 mm specimens. The fabrication processes of the specimens are shown in Fig. 1, and the dimensions of the eight types of CLT specimens are listed in Tables 1 and 2.

Figure 2 shows all the metal connectors and fasteners used in this study. The tests were conducted at the mechanics laboratory of the Yangzhou Institute of Industry and Technology (Yangzhou, China). The bolt shear failure test was conducted using a WDW-200 micro-controlled electronic universal testing machine developed by Nanjing UP Electronic Technology Co., Ltd. (Nanjing, China). The maximum loading force of the horizontal load was 200 kN. As shown in Fig. 3, the bolt connection CLT specimens were connected to angle brackets by one 8.8 grade high-strength bolt with a diameter of 10 mm and length of 100 mm. Meanwhile, the screw connection CLT specimens were connected to two steel plates with eight screws (four on each side).


**Fig. 2.** Metal connectors and fasteners used in the tests

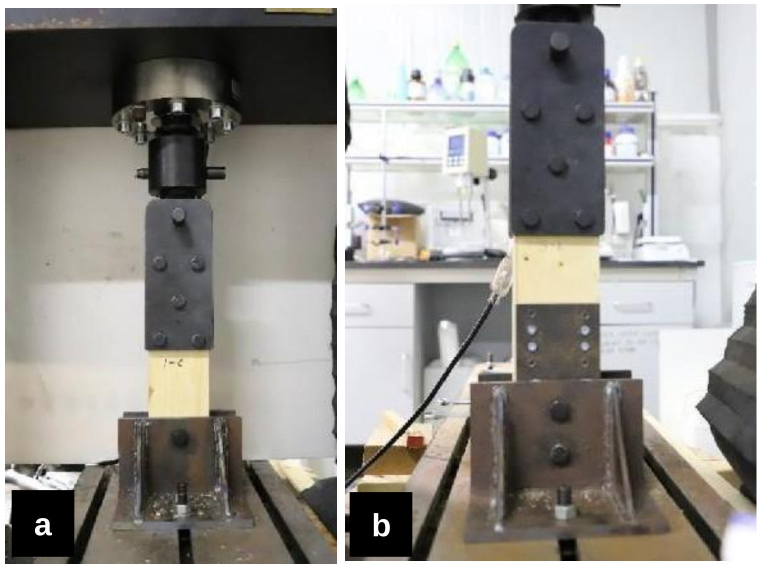


**Fig. 3.** Experimental setup for a shear test of CLT specimens: (a) setup for bolt connection specimens and (b) setup for screw connection specimens

The steel plates were connected to angle brackets by two 8.8 grade high-strength bolts. The angle bracket and the underlying steel beam were connected by one 8.8 grade high-strength bolt with a diameter of 20 mm and length of 60 mm. All the nuts were finger-tight. After the specimen was installed, the loading head was moved slightly upward to tighten the specimen.

## Methods

The bolt shear test was conducted as per ASTM D1761-12 (2020). After the specimen was installed, the loading head was moved slightly upward to eliminate the gap error of the mounting hole. After the test started, the loading head was moved upward at a rate of 5 mm/min and stopped when the bearing capacity dropped to 80% of the ultimate load or obvious damage occurred (ASTM D1761-12 2020).

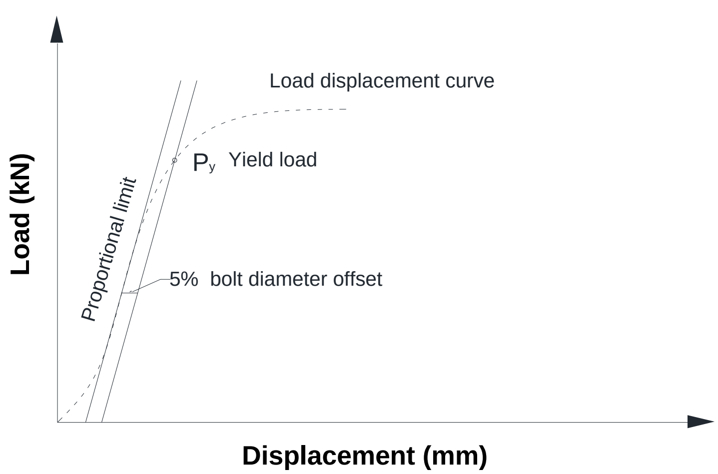


**Fig. 4.** Typical load-displacement curve for bolt and screw connection

The elastic stiffness $K$, ultimate bearing capacity $P_{max}$, corresponding displacement $\Delta_{max}$, yield displacement $\Delta_y$, and ductility coefficient $D$ can be obtained based on the load-displacement curves from the test, $D = \Delta_{max}/\Delta_y$. In particular, $P_{max}$ and $\Delta_{max}$ were taken from the peak point of the load-displacement curve. According to ASTM D1761-12 (2020), the slope of the linear part of the load-displacement curve represents the $K$ value, obtained using a two-point line of 10% $P_{max}$ and 40% $P_{max}$ of the load-displacement curve. According to the American NDS-2012 standard (2012), the linear part of the initial curve is offset by 5% of the bolt or screw diameter, and the intersection of the line and the curve represents the yield load $P_y$.

## RESULTS AND DISCUSSION

### Failure Modes

Figure 5 shows the bolts after the test. Almost no bending occurred in the bolts. Figure 6 shows the deformation and failure of the screws after the test.


**Fig. 5.** Deformation of the bolts after the test: (a) bolts of type 1 specimens, (b) bolts of type 2 specimens, (c) bolts of type 3 specimens, and (d) bolts of type 4 specimens

Considering the specimen types in Table 2, when the screw length was 60 mm, the screw deformation of type 6 specimens, whose outer-layer wood grain direction was perpendicular to the load direction, was larger, and bending occurred in the middle of the screws. The bending deformation of screws in the type 6 specimens, whose outer-layer wood grain direction was parallel to the load direction, occurred near the screw head. When the screw length was 40 mm, the specimens whose outer-layer wood grain direction was parallel to the load direction underwent obvious bending deformation, and all specimens exhibited shear failure. In contrast, the specimens whose outer-layer wood grain direction was perpendicular to the load direction exhibited nearly no deformation when the specimens were destroyed.


**Fig. 6.** Deformation and failure of the screws after the test: (a) screws of type 5, (b) screws of type 6, (c) screws of type 7, and (d) screws of type 8

Figure 7 shows the failure modes of bolt holes of the bolt connection CLT specimens. As shown in Figs. 7(a) and (b), when the outer-layer grain direction of the CLT panel was parallel to the load direction and the distance between the bolt hole and the bottom of the specimen was 40 mm, the destruction of the CLT panel around the bolt hole was wood crushing and block shear (see red arrow in the figure). Furthermore, there were no obvious signs of damage in the middle layer of the CLT panel.

When the bolt hole was 70 mm away from the bottom (type 2 specimen), a large collapse failure occurred below the bolt hole, and the block shear of the middle layer of the CLT panel was observed from the side of the specimen. When the outer-layer grain direction of the CLT panel was perpendicular to the load direction, the transverse layers on both sides exhibited obvious transverse cracking failure.

The damage degree of the type 3 specimen, whose bolt hole was 40 mm from the bottom, was noticeably greater than that of the specimen whose bolt hole was 70 mm from the bottom. In addition, when the bolt hole margin was 40 mm, obvious block shear occurred at the bottom of the middle layer of the CLT panel. The red circle in Fig. 7(c) denotes the block shear.

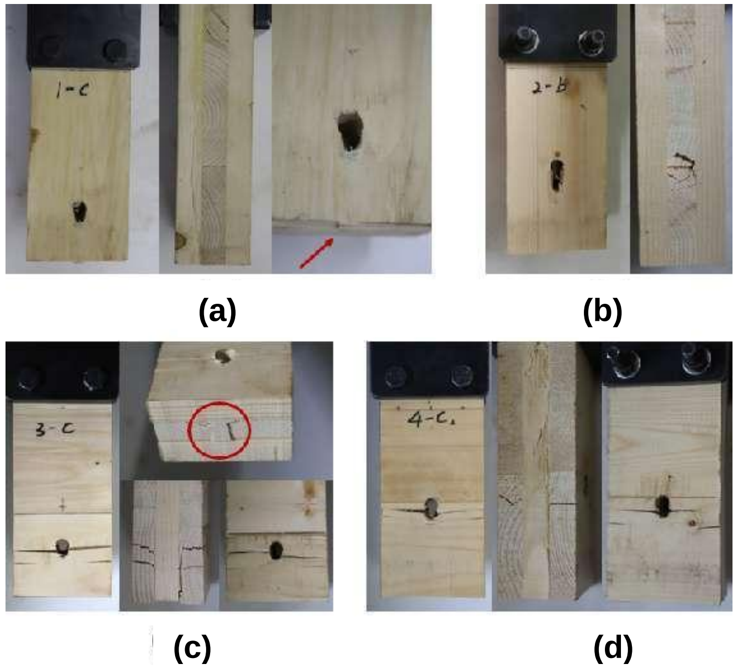


**Fig. 7.** Typical failure appearances of the bolt connection CLT specimens during the shear tests: (a) type 1; (b) type 2; (c) type 3; (d) type 4

Figure 8 shows the failure modes of the screw connection CLT specimens. Figures 8(a) and (b) show the failure modes of specimens that employed 60-mm screws. The specimens with an outer-layer wood grain direction parallel to the load direction exhibited wood crushing under the screw holes and splitting in the vertical direction. When viewed from the side, the middle layers of some specimens had microscopic cracks. When the outer-layer wood grain direction was perpendicular to the load direction, obvious horizontal cracks were observed in the positions of the screw holes, and the size of the screw holes did not increase noticeably. Further, many cracks were observed on the sides of the specimens. Figures 8(c) and (d) show the failure modes of specimens with 40-mm screws. When the outer-layer wood grain direction of the specimens was parallel to the load direction, the failure mode was similar to that of the specimens with 60-mm screws. When the outer-layer wood grain direction was perpendicular to the load direction, the main failure mode was horizontal cracking around the screw holes, and the cracking degree was lower than that of the specimens with 60-mm screws. When viewed from the side, the adhesive layer between the outer and middle layers around the screw holes was damaged, which eventually caused the outer layer to fall off.

The failure modes of the bolt and screw connection CLT specimens are comprehensively compared as follows. First, from the perspective of deformation and failure of the metal connector, the bolts had no obvious deformation, whereas the screws had obvious deformation, except for the screws in the type 8 specimens; most of the specimens exhibited shear failure in one to three screws. Second, the failure of the specimens connected by screws was more severe. When the outer-layer wood grain direction was parallel to the load direction, the failure of the bolt connection specimens manifested as wood collapse below the bolt hole, while the screw connection specimens had a certain probability of cracking along the wood grain direction when the wood collapse occurred below the screw hole. When the outer-layer wood grain direction was perpendicular to the load direction, both the bolt hole and the screw hole produced transverse cracks along the grain. The cracks in the screw connection specimens were longer and were often transverse throughout the specimens. In addition, the outer-layer wood cracks in the screw connection specimens were more severe than those in the bolt connection specimens when viewed from the side. The outer layer of the specimens connected by 40-mm screws eventually fell off. In general, the bolt connection CLT panels were more likely to be repaired after breakage and had a higher rate of reuse than the screw connection CLT panels.

By comprehensively comparing the failure modes of metal connectors and wood in the two connections, it can be found that the bolts had no obvious failure when bolt connection was used, and the wood failure area was smaller and concentrated, which indicated that the connection part of the bolt connection CLT shear wall had better repairability.

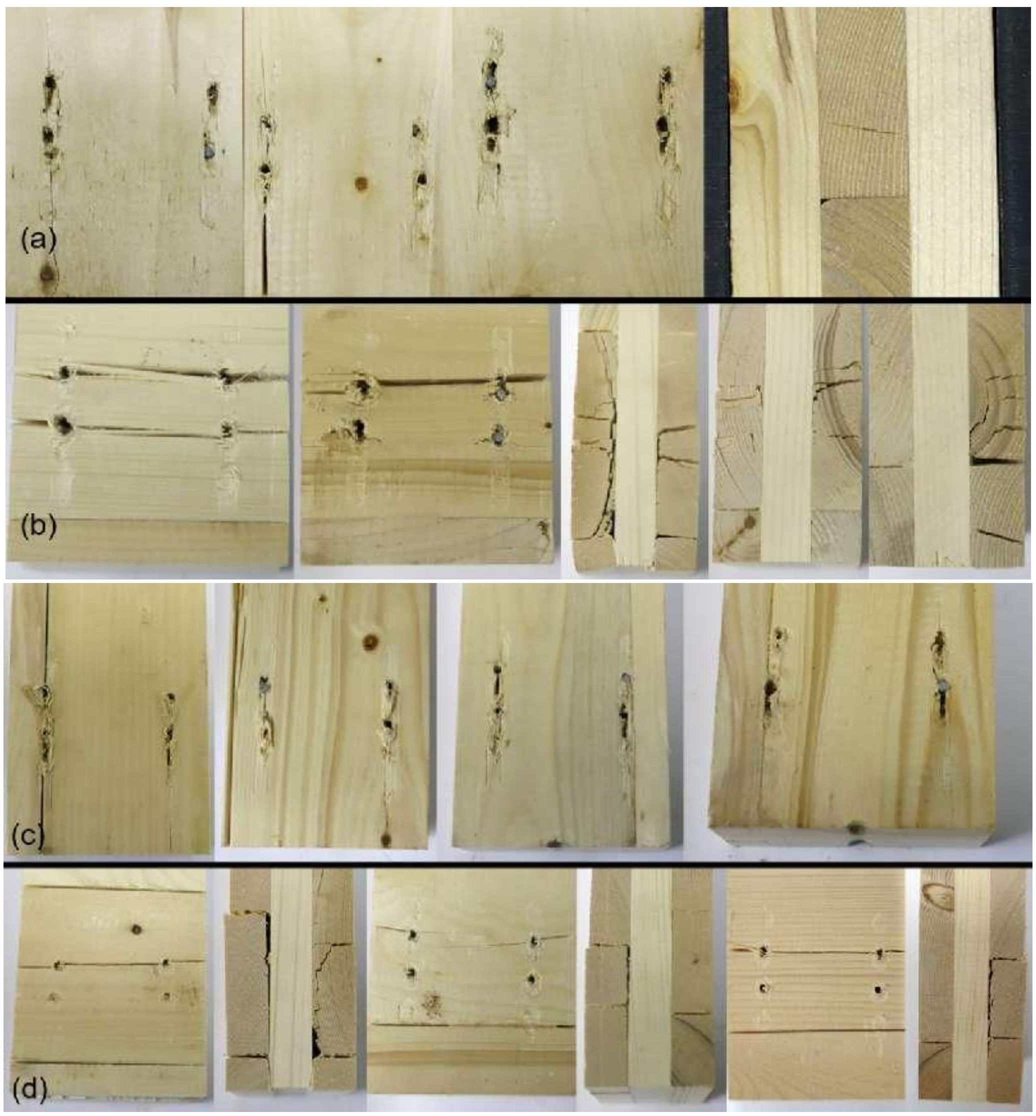


**Fig. 8.** Typical failure appearances of the screw connection CLT specimens during the shear tests: (a) type 5; (b) type 6; (c) type 7; and (d) type 8

## Mechanical Properties

Table 3 summarizes the test data and calculated performance indexes of all 24 specimens. Figure 9 shows the average ultimate bearing capacity ($P_{max}$) and yield load ($P_y$) of the eight types of CLT specimens. When the specimens were connected by bolts, the $P_{max}$ of types 1 and 2 specimens, whose outer-layer wood grain direction was parallel to the load direction, was noticeably greater than that of type 3 and type 4 specimens, whose outer-layer wood grain direction was perpendicular to the load direction. When the distance (*d*) between the bolt hole and the bottom of the specimen was 40 mm, the $P_{max}$ of type 1 increased 13.9% while $P_y$ increased 19.3% compared with type 3. When *d* was 70 mm, the $P_{max}$ and $P_y$ of type 2 were 31.6% and 51.8% greater than those of type 4, respectively. The increase was more obvious when *d* was 70 mm because the rest of the wood under the bolt hole was more prone to shear failure after being crushed when *d* was 40 mm. When *d* was changed from 40 mm to 70 mm, the $P_{max}$ and $P_y$ of specimens whose outer-layer wood grain direction was parallel to the load direction increased more obviously, up to 28.2% and 21.8%, respectively. However, the $P_{max}$ of specimens whose outer-layer wood grain direction was perpendicular to the load direction increased only 10.9%, whereas $P_y$ decreased 4.2%. This indicated that the failure of the specimens when the outer-layer wood grain direction was perpendicular to the load direction depended on the tensile strength of the transverse grain on both sides of the bolt hole.

When the specimens were connected by screws, the $P_{max}$ of the specimens with 60 mm screws was noticeably greater than that of the specimens with 40-mm screws. When the outer-layer wood grain direction was parallel to the load direction, the $P_{max}$ of the specimens with 60-mm screws increased 50.9% compared with that of the specimens with 40-mm screws. When the outer-layer wood grain direction was perpendicular to the load direction, this value increased 133.9%. Thus, when the CLT panels were connected with the screws, the depth of the screw penetration into the panels had a noticeably impact on the shear performance of the connection. When the 60-mm screw was used, the direction of the outer-layer wood grain did not have a noticeable effect on the test results, and the $P_{max}$ and $P_y$ of type 5 and type 6 specimens increased 4.6% and 8.3%, respectively. However, when the 40-mm screw was used, the values for the specimens whose outer-layer wood grain direction was parallel to the load direction were obviously greater than those for the specimens whose outer-layer wood grain direction was perpendicular to the load direction; $P_{max}$ and $P_y$ increased 62.1% and 38.3%, respectively. Considering the failure mode of the screw connection specimens in Fig. 8, in the specimens that employed 40 mm screws with the outer-layer wood grain direction perpendicular to the load direction, the depth of the screw penetration into the specimen was small. Therefore, the pull force of the screw acted on the outer layer of wood, resulting in separation and failure of the outer layer at the position of the screw hole.

By comparing type 2 specimens with the best performance in bolt connection and type 5 specimens with the best performance in screw connection, it can be found that the $P_{max}$ and $P_y$ of type 5 specimens were 12% and 11% higher than that of type 2 specimens, respectively. Although the bearing capacity of test piece No. 5 was higher, the total amount of steel used by 8 screws was about 1.3 times that of 1 bolt. Therefore, the bolt connection is reliable, easy to disassemble and saves material.

**Table 3.** Mechanical Properties of All CLT Specimens

| | $K$ (kN/mm) | $P_{max}$ (kN) | $P_y$ (kN) | $\Delta_y$ (mm) | $\Delta_{max}$ (mm) | $D$ |
|---|---|---|---|---|---|---|
| 1-a | 2.9 | 15.1 | 14.4 | 6.8 | 7.9 | 1.3 |
| 1-b | 2.9 | 14.8 | 12.0 | 5.7 | 13.2 | 2.3 |
| 1-c | 2.6 | 16.8 | 16.1 | 6.3 | 7.8 | 1.2 |
| 2-a | 3.2 | 21.4 | 18.9 | 8.8 | 24.8 | 2.8 |
| 2-b | 3.1 | 18.4 | 15.2 | 8.1 | 24.4 | 3.0 |
| 2-c | 3.6 | 20.1 | 17.8 | 6.8 | 23.2 | 3.4 |
| 3-a | 2.4 | 18.8 | 16.0 | 6.8 | 10.2 | 1.5 |
| 3-b | 2.4 | 11.5 | 10.1 | 7.5 | 7.9 | 1.1 |
| 3-c | 2.1 | 10.8 | 9.6 | 6.1 | 9.5 | 1.6 |
| 4-a | 2.6 | 14.2 | 11.1 | 5.4 | 8.9 | 1.6 |
| 4-b | 2.9 | 15.6 | 10.9 | 7.1 | 21.1 | 3.0 |
| 4-c | 2.3 | 15.9 | 12.2 | 5.1 | 14.8 | 2.9 |
| 5-a | 2.5 | 28.4 | 25.3 | 16.7 | 19.6 | 1.2 |
| 5-b | 2.2 | 24.7 | 18.0 | 13.9 | 19.0 | 1.4 |
| 5-c | 2.4 | 22.4 | 19.2 | 14.2 | 17.4 | 1.2 |
| 6-a | 2.1 | 21.5 | 17.1 | 15.1 | 20.6 | 1.4 |
| 6-b | 1.8 | 26.0 | 22.1 | 19.2 | 23.7 | 1.2 |
| 6-c | 2.2 | 24.8 | 18.4 | 16.2 | 20.6 | 1.3 |
| 7-a | 1.5 | 14.7 | 10.4 | 12.3 | 21.4 | 1.7 |
| 7-b | 1.9 | 19.2 | 17.3 | 16.3 | 20.5 | 1.3 |
| 7-c | 1.9 | 16.1 | 11.2 | 11.2 | 17.5 | 1.6 |
| 8-a | 1.3 | 9.1 | 8.7 | 13.7 | 14.5 | 1.1 |
| 8-b | 1.6 | 12.4 | 10.9 | 12.6 | 14.6 | 1.2 |
| 8-c | 1.1 | 9.5 | 8.6 | 12.6 | 13.5 | 1.1 |

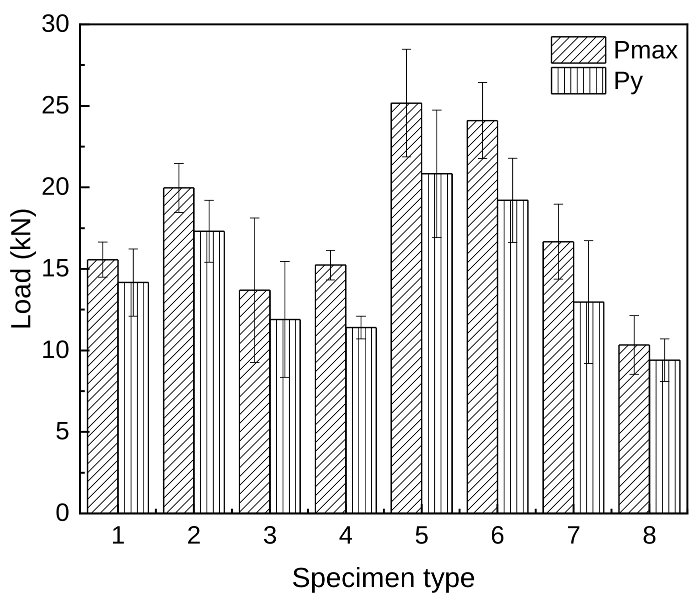


**Fig. 9.** Peak load ($P_{max}$) and yield load ($P_y$) of the eight types of CLT specimens

Figure 10 shows the average elastic stiffness *K* and ductility coefficient *D* of all the specimens. Figure 13 shows the load-displacement curves of the bolt and screw specimens of each type after averaging. First, a comparison of the *K* and *D* values of the bolt and screw connection specimens shows that the *K*-mean and *D*-mean of the bolt connection specimens were 2.8 and 2.2, respectively. Further, the *K*-mean and *D*-mean of the screw connection specimens were 1.9 and 1.3, respectively. Thus, although the bolt connection CLT panels showed better elastic stiffness, they mainly suffered from brittle failure; hence, the ductility coefficient of the bolt connection specimens was relatively low. From observing the separate analysis of the bolt connection specimens, when the CLT panels were connected by bolts, the specimens whose outer-layer wood grain direction was parallel to the load direction had higher elastic stiffness and a larger ductility coefficient. Meanwhile, the elastic stiffness and ductility coefficient of specimens with a *d* value of 70 mm were noticeably higher than those with a *d* value of 40 mm. Among the four types of specimens connected by screws, the elastic stiffness of specimens with 60-mm screws was noticeably higher than that of specimens with 40-mm screws; however, the screw length had no noticeable effect on the ductility coefficient of the specimens (1.3 on average). This may have been due to the brittle failure of the CLT specimens connected by screws when they reached the ultimate load.

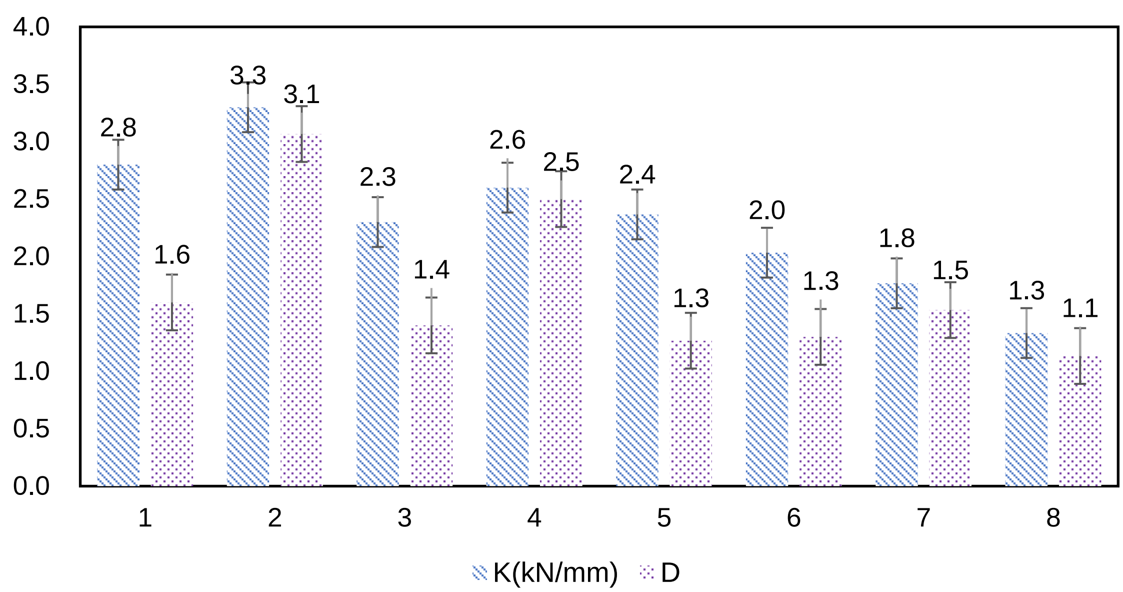


**Fig. 10.** *K* and *D* of the eight types of CLT specimens

The loading displacement curves of the eight types of specimens show that the slope of the bolt connection specimens was higher than that of the screw connection specimens in the elastic stage, which implied a larger elastic stiffness. Bolt connection specimens with a *d* value of 40 mm showed obvious brittle failure characteristics after reaching $P_{max}$, especially type 3 specimens whose outer-layer wood grain direction was perpendicular to the load direction. The load-displacement curves of type 2 and type 4 specimens, whose *d* value was 70 mm, showed an obvious plastic stage after the elastic stage, and the load increased gradually with the displacement. Considering the failure mode in Fig. 7, the plastic stage in the curve was deformation caused by the continuous crushing of the wood below the bolt hole.

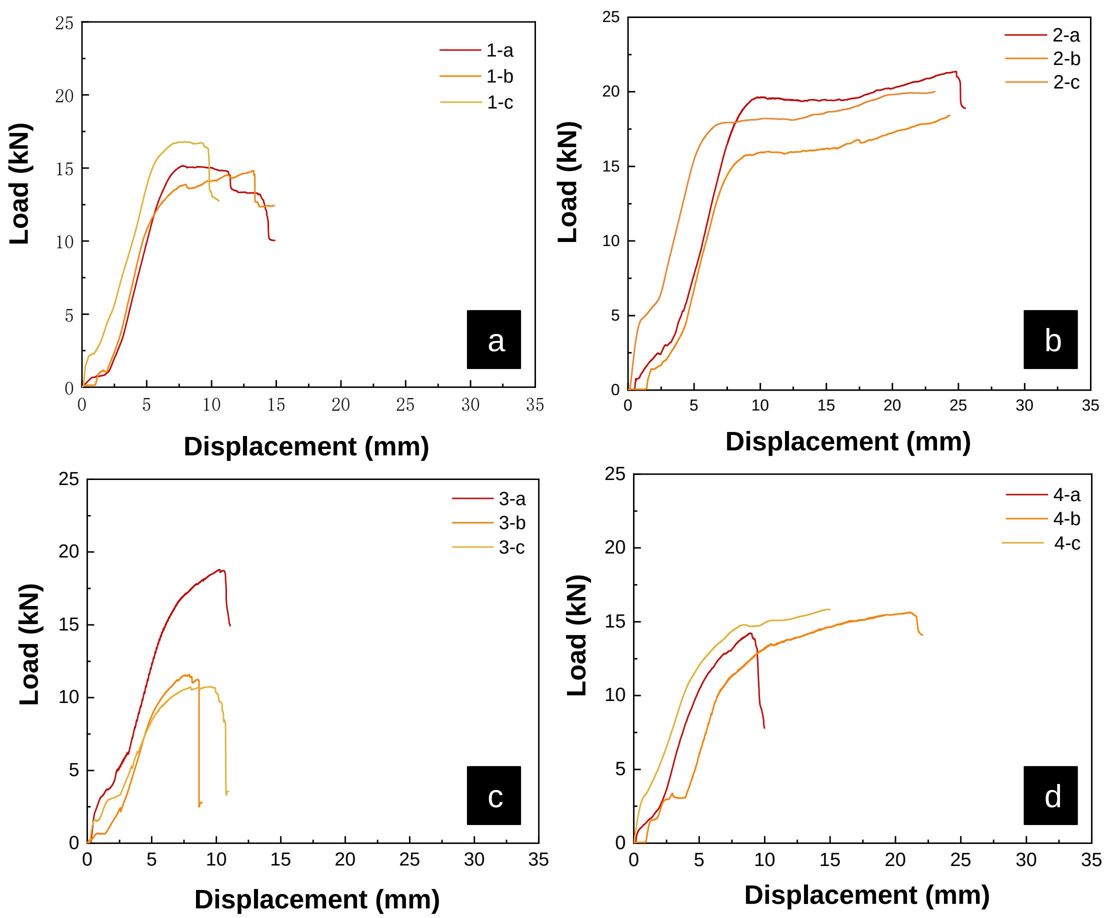


**Fig. 11.** Load-displacement curves of bolt connection CLT specimens: (a) curves of type 1 specimens, (b) curves of type 2 specimens, (c) curves of type 3 specimens, and (d) curves of type 4 specimens

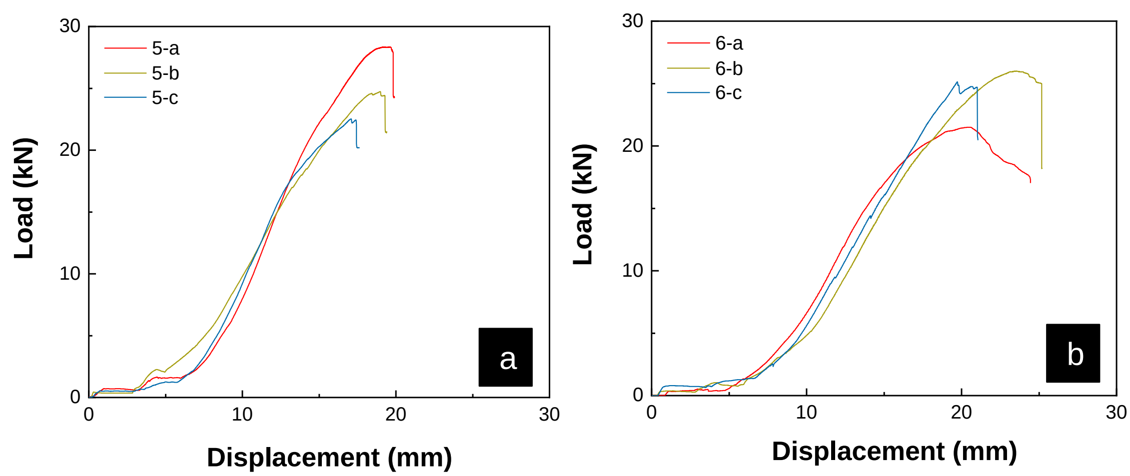


**Fig. 12.** Load-displacement curves of screw connection CLT specimens: (a) curves of type 5 specimens, (b) curves of type 6 specimens, (c) curves of type 7 specimens, and (d) curves of type 8 specimens

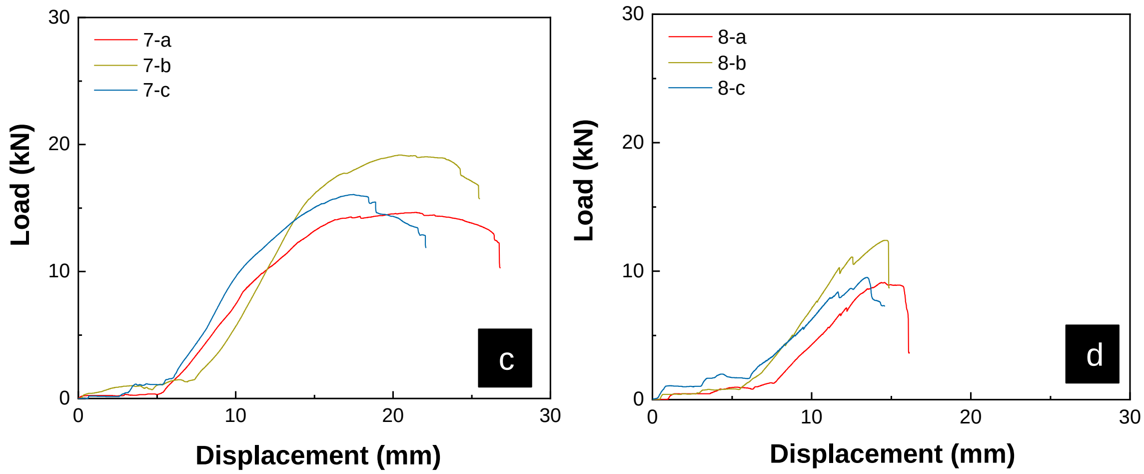


**Fig. 12 cont.** Load-displacement curves of screw connection CLT specimens: (a) curves of type 5 specimens, (b) curves of type 6 specimens, (c) curves of type 7 specimens, and (d) curves of type 8 specimens

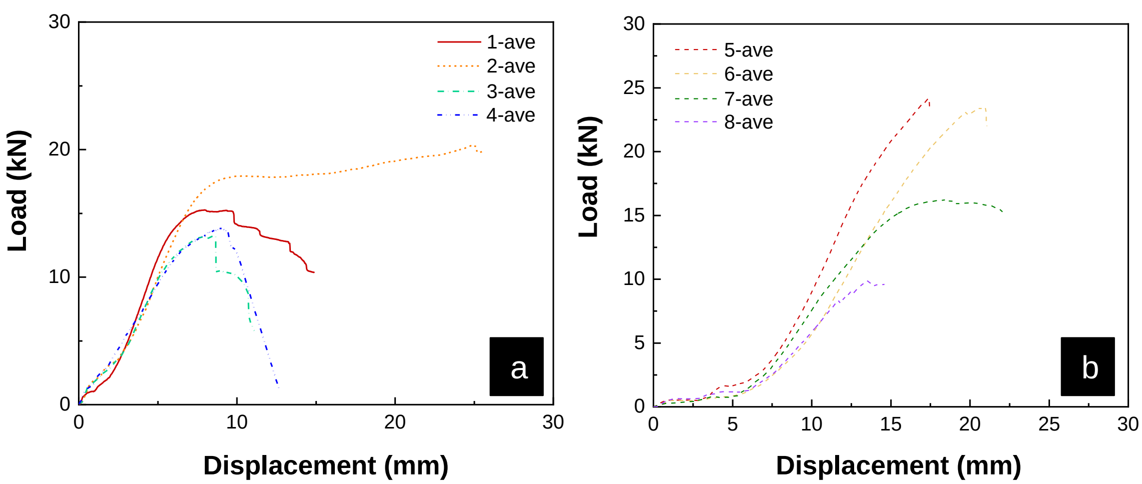


**Fig. 13.** Average load-displacement curves of CLT specimens: (a) curves of bolt connection specimens and (b) curves of screw connection specimens

The greater density of the crushed wood led to a further increase in the load until shear failure of the wood below the bolt hole occurred. According to the average load-displacement curve of the screw connection specimens, the screw length had a noticeable effect on the ultimate bearing capacity and elastic stiffness of the specimens, and the elastic stiffness of the specimens employing 40-mm screws was noticeably lower. The load-displacement curves of all the screw connection specimens except for the type 7 specimens showed brittle failure.

The plastic phase of the curve for the type 7 specimens could be attributed to the fact that as the displacement increased, the screw was pulled out simultaneously with the shearing, resulting in an increase in displacement and a slight change in load.

## CONCLUSIONS

1. A comparison of the bolt and screw connection cross-laminated timber (CLT) panels showed that the bolts exhibited no obvious deformation when the specimens were destroyed, whereas the screws exhibited large deformation or were even cut off. Meanwhile, the damage to the CLT panel in the screw connection specimens was more severe than that in the bolt connection specimens. Combining these two aspects, it is concluded that a bolt connection CLT structure has better repairability.
2. A comparison of the $P_{max}$ and $K$ values of the bolt and screw connection specimens showed that in terms of $P_{max}$, the bolt connection specimen with a $d$ value of 70 mm and the screw connection specimen with a screw length of 60 mm achieved better performance. There was no noticeable difference between these two cases in terms of $P_{max}$. However, the bolt connection specimens had a noticeably larger elastic stiffness than the screw connection specimens. Therefore, bolt connection specimens improved the lateral stiffness of CLT walls more effectively.
3. The experimental results showed that the screw length had an obvious effect on the ultimate bearing capacity and elastic stiffness of the screw connection CLT panels, whereas it did not have a noticeable effect on the ductility coefficient. When the screw length was 60 mm, the shear strength of the specimens was close to that of the bolt connection specimens under the same section; however, when the screw length was 40 mm, each screw was able to pass through only one layer of the CLT panel, resulting in an obvious decrease in the connection strength. When the outer-layer wood grain direction of the specimen is perpendicular to the load direction, the screw connection will fail rapidly and cause the outer layer of the CLT panel to fall off.
4. For the bolt connection specimens, the shear strength was greater when the outer-layer grain direction of the CLT panel was parallel to the load direction, and the difference was greater when the distance between the bolt hole and the bottom of the specimen was 70 mm. The increase in $P_{max}$ and $P_y$ was 31.6% and 51.8%, respectively. When the outer-layer wood grain direction of the CLT panel specimen was parallel to the load direction, the distance between the bolt hole and the bottom of the specimen increased from 40 mm to 70 mm, which noticeably improved the shear strength of the bolt connection. The peak load and yield load of type 2 specimens increased 28.2% and 21.8%, respectively, compared with type 1 specimens. For specimens whose outer-layer wood grain direction was perpendicular to the load direction, there was no obvious change; the yield load of type 4 specimens decreased 4.2% compared with type 3 specimens.

## ACKNOWLEDGMENTS

The authors are grateful for the support of a Project Funded by the Priority Academic Program Development of Jiangsu Higher Education Institutions (PAPD), the National Natural Science Foundation of China (Grant No. 31901252), the Qing Lan Project of Jiangsu, the Yangzhou Science and Technology Project (Grant No. YZ2020203), and the Science and Technology Program of Jiangsu Housing and Construction Department

(Grant No. 2020ZD43). The authors would like to thank TopEdit (www.topeditsci.com) for its linguistic assistance during the preparation of this manuscript.

## REFERENCES CITED

ASTM D1761-12 (2020). "Standard test methods for mechanical fasteners in wood and wood-based materials," ASTM International, West Conshohocken, PA, USA.

Brandner, R., Flatscher, G., Ringhofer, A., Schickhofer, G., and Thiel, A. (2016). "Cross laminated timber (CLT): Overview and development," *European Journal of Wood and Wood Products* 74, 331-351. DOI: 10.1007/s00107-015-0999-5

CSA O86-14 (2019). "Engineering design in wood," CSA Group, Toronto, Canada.

Daudeville, L., Davenne, L., and Yasumura, M. (1999). "Prediction of the load carrying capacity of bolted timber joints," *Wood Science and Technology* 33, 15-29. DOI: 10.1007/s002260050095

Dinehart, D. W., and Shenton, III, H. W. (2000). "Model for dynamic analysis of wood frame shear walls," *Journal of Engineering Mechanics* 126(9), 899-908. DOI: 10.1061/(ASCE)0733-9399(2000)126:9(899)

Frangi, A., Fontana, M., Hugi, E., and Jübstl, R. (2009). "Experimental analysis of cross-laminated timber panels in fire," *Fire Safety Journal* 44(8), 1078-1087. DOI: 10.1016/j.firesaf.2009.07.007

Frangi, A., Fontana, M., Knobloch, M., and Bochicchio, G. (2008). "Fire behaviour of cross-laminated solid timber panels," *Fire Safety Science* 9, 1279-1290. DOI: 10.3801/IAFSS.FSS.9-1279

IEA. (2019). "Global Status Report for Buildings and Construction 2019," IEA, Paris.

Kharouf, N., McClure, G., and Smith, I. F. (2005). "Postelastic behavior of single- and double-bolt timber connections," *Journal of Structural Engineering* 131(1), 188-196. DOI: 10.1061/(ASCE)0733-9445(2005)131:1(188)

Klippel, M., Leyder, C., Frangi, A., Fontana, M., Lam, F., and Ceccotti, A. (2014). "Fire tests on loaded cross-laminated timber wall and floor elements," *Fire Safety Science* 11, 626-639. DOI: 10.3801/IAFSS.FSS.11-626

Li, M., Foschi, R. O., and Lam, F. (2012). "Modeling hysteretic behavior of wood shear walls with a protocol-independent nail connection algorithm," *Journal of Structural Engineering* 138, 99-108. DOI: 10.1061/(ASCE)ST.1943-541X.0000438

Li, Z., Xiao, Y., Wang, R., and Monti, G. (2015). "Studies of nail connectors used in wood frame shear walls with ply-bamboo sheathing panels," *Journal of Materials in Civil Engineering* 27(7), article ID 04014216. DOI: 10.1061/(ASCE)MT.1943-5533.0001167

Moses, D. M., and Prion, H. G. (2003). "A three-dimensional model for bolted connections in wood," *Canadian Journal of Civil Engineering* 30(3), 555-567. DOI: 10.1139/l03-009

NDS-2012 (2012). "National design specification for wood construction," American Forest and Paper Association, Washington D.C., USA.

Richard, N., Daudeville, L., Prion, H. G., and Lam, F. (2002). "Timber shear walls with large openings: Experimental and numerical prediction of the structural behaviour," *Canadian Journal of Civil Engineering* 29(5), 713-724. DOI: 10.1139/l02-050

Schickhofer, G., and Guggenberger, W. (1994). "Elastic analysis of flexibly jointed laminated timber plates," in: 1st Congress of Croatian Society of Mechanics, Pula 14-17 Sept 1994: Conference Proceedings.

Sikora, K. S., McPolin, D. O., and Harte, A. M. (2016). "Effects of the thickness of cross-laminated timber (CLT) panels made from Irish Sitka spruce on mechanical performance in bending and shear," *Construction and Building Materials* 116, 141-150. DOI: 10.1016/j.conbuildmat.2016.04.145

Varoḡlu, E., Karacabeyli, E., Stiemer, S. F., Ni, C., Buitelaar, M., and Lungu, D. (2007). "Midply wood shear wall system: Performance in dynamic testing," *Journal of Structural Engineering* 133(7), 1035-1042. DOI: 10.1061/(ASCE)0733-9445(2007)133:7(1035)

Verdret, Y., Faye, C., Elachachi, S. M., Le Magorou, L., and Garcia, P. (2015). "Experimental investigation on stapled and nailed connections in light timber frame walls," *Construction and Building Materials* 91, 260-273. DOI: 10.1016/j.conbuildmat.2015.05.052

Wang, Z., Gong, M., and Chui, Y.-H. (2015). "Mechanical properties of laminated strand lumber and hybrid cross-laminated timber," *Construction and Building Materials* 101(Part 1), 622-627. DOI: 10.1016/j.conbuildmat.2015.10.035

Wei, Z., Lu, W., Liu, W., Wang, L., and Ling, Z. (2015). "Experimental investigation of laterally loaded double-shear-nail connections used in midply wood shear walls," *Construction and Building Materials* 101(Part 1), 761-771. DOI: 10.1016/j.conbuildmat.2015.10.100

Article submitted: April 27, 2022; Peer review completed: September 3, 2022; Revised version received and accepted: November 22, 2022; Published: December 2, 2022.
DOI: 10.15376/biores.18.1.827-843